Electronic Supplementary Material (ESI) for Chemical Communications.

Enhanced stereoselectivity in a di-Ru(II) complex of an achiral bis-bidentate ligand

Amlan K. Pal,[a] Philippe D. Ducharme,[a] Garry S. Hanan*,[a]

[a]*Département de Chimie, Université de Montréal, 2900 Edouard-Montpetit, Montréal, Québec H3T-1J4, Canada.*

Electronic Supporting Information

Materials, methods and instrumentation

Nuclear magnetic resonance (NMR) spectra were recorded in CD_3CN at room temperatutre (r.t.) on a Bruker AV400 (400 MHz) and AV700 (700 MHz) spectrometers (as noted in the experimental) for ^{1}H-NMR and at 100 and 175 MHz (as noted in the experimental) for ^{13}C NMR, respectively. Chemical shifts are reported in part per million (ppm) relative to residual solvent protons (1.94 ppm for CD_3CN, 7.26 ppm for $CDCl_3$) and the carbon resonance (118.69 ppm for CD_3CN, 77.00 ppm for $CDCl_3$) of the solvent.

Absorption spectra were measured in deaerated acetonitrile at r.t. on a Cary 500i UV-Vis-NIR Spectrophotometer. Electrochemical measurements were carried out in argon-purged purified acetonitrile at room temperature with a BAS CV50W multipurpose equipment interfaced to a PC. The working electrode was a glassy carbon electrode. The counter electrode was a Pt wire, and the pseudo-reference electrode was a silver wire. The reference was set using an internal 1 mM ferrocene/ferrocinium sample at 395 mV vs SCE in acetonitrile. The concentration of the compounds was about 1 mM. Tetrabutylammonium hexafluorophosphate (TBAP) was used as supporting electrolyte and its concentration was 0.10 M. Cyclic voltammograms of **L1** and **1**(***meso***) were obtained at scan rates of 100 and 25 mv/s, respectively. The criteria for reversibility were the separation of 60 mV between cathodic and anodic peaks, the close to unity ratio of the intensities of the cathodic and anodic currents, and the constancy of the peak potential on changing scan rate. Differential pulse voltammetry was conducted with a sweep rate of 20 mVs−1 and a pulse amplitude, width and period of 50 mV, 50 ms and 200 ms, respectively.

Experimental uncertainties are as follows: absorption maxima, ±2 nm; molar absorption coefficient, 10%; redox potentials, ± 10 mV.

1,3,4,6,7,8-Hexahydro-2*H*-pyrimido[1,2-*a*]pyrimidine (**H-hpp**), 4,6-dichloropyrimidine, $AgNO_3$, and KPF_6 were purchased from Aldrich as used as received. *Cis*-$Ru(bpy)_2Cl_2$.$2H_2O$ was synthesized using standard literature procedure.[1]

Experimental:

Synthesis of ligand **L1** (**dgpm**):

4,6-bis-[1,3,4,6,7,8-Hexahydro-2*H*-pyrimido[1,2-*a*]pyrimidine]pyrimidine (L1) (dgpm): 4,6-Dichloropyrimidine (2 mmol, 0.307 g) and 1,3,4,6,7,8-hexahydro-2H-pyrimido[1,2-a]pyrimidine (**H-hpp**) (4 eq, 8 mmol, 1.126 g) were combined in toluene (20 mL) in a microwave vial. The tube was sealed and placed in a Biotage 400 MW microwave reactor. The suspension was heated to 160 °C for 2 hours, after which time the solution was slowly decanted out and evaporated to dryness. The crude product could be purified by overnight sublimation at 1.8 mbar and 100 °C, as colourless crystals (**L1**). Yield = 638 mg (90%). ^{1}H-NMR: (400 MHz, $CDCl_3$) (see Scheme S1 for numbering) δ ppm 8.43 (s, 1 H_1), 8.21 (s, 1 H_3), 3.96 (t, J^t = 6 Hz, 4 H_4), 3.46 (t, J^t = 6 Hz, 4 H_9), 3.22 (t, J^t = 6 Hz, 4 H_7), 3.14 (t, J^t = 6 Hz, 4 H_6), 1.97 (quint, J^{qt} = 6 Hz, 4 H_5), 1.89 (quint, J^{qt} = 6 Hz, 4 H_8). ^{13}C-NMR: (100 MHz, $CDCl_3$) δ ppm 160.9 (C_2), 156.7 (C_1), 148.9 (C_3), 98.9 (C_{10}), 48.7 (C_7), 48.7 (C_6), 43.9 (C_9), 42.4 (C_4), 23.8 (C_8), 22.6 (C_5). HRMS (ESI), m/z: 355.23635 $[M+H^+]^+$ ($C_{18}H_{27}N_8$ requires 355.23532). Anal. Calc. for $C_{18}H_{26}N_8$: C: 60.99; N: 31.61; H: 7.39. Found: C: 60.75; N: 31.70; H: 7.35. Melting point: 182-185 °C.

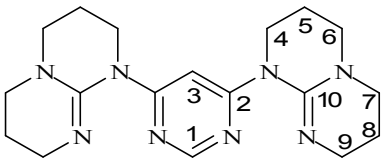

Scheme S1: Numbering of protons and carbons of compound **L1**.

Synthesis of the complex **1**(***meso***):

*Meso-[{Ru(bpy)$_2$}$_2$(μ-**L1**)](PF$_6$)$_4$* (**1**(***meso***)):

A 250 mL round-bottomed flask was charged with *cis*-Ru(bpy)$_2$Cl$_2$ .2H$_2$O (0.513 g, 0.987 mmol), AgNO$_3$ (0.344 g, 2.025 mmol, 2.05 eq) in methanol (150 mL). The suspension was heated to reflux for 3 hours to give a dark red solution with a white precipitate of AgCl. The solution was cooled down to room temperature and then filtered through a plug of celite and was washed with methanol (3x30 mL). Filtrate and washings were collected and evaporated to dryness to give a dark red solid. To this solid was added **L1** (0.100 g, 0.282 mmol), followed by the addition of *n*-BuOH (150 mL) and the suspension was heated to reflux, under N$_2$-atmosphere for 16 h. After this time, the solution was cooled down to room temperature and evaporated to dryness. The crude product was purified through a silica column using 7:1 = CH$_3$CN:saturated aq. KNO$_3$ solution (v/v) as an eluant and then increasing the polarity of the eluent to 7:2:1 = CH$_3$CN:saturated aq. KNO$_3$ solution:H$_2$O (v/v/v). The slowest moving and major dark red band was collected, solvent was evaporated to dryness and the NO_3^- salt was metathesised to PF_6^- salt by addition of saturated aqueous KPF$_6$ solution. The dark red solid was collected by filtration was dried under vacuum to furnish the product, which could be recrystallised from a concentrated acetonitrile solution by diffusing diethylether into it. Yield = 0.325 g (65%). ^{1}H NMR (700 MHz, ACETONITRILE-d_3) δ ppm 1.05 (m, 2 H), 1.61 (m, 2 H), 2.04 (m, 2 H), 2.11 (m, 2 H), 2.29 (m, 2 H), 2.89 (m, 2 H), 3.02 (quint, J^{qt} = 6 Hz, 2 H), 3.17 (m, 6 H), 3.37 (m, 2 H), 3.95 (m, 2 H), 6.18 (s, 1 H), 6.87 (s, 1 H), 6.97 (t, J^t = 8 Hz, 2 H), 7.10 (m, 6 H), 7.56 (m, 4 H), 7.81 (dt, J^{dt} = 8, 2.0 Hz, 2 H), 7.89 (dt, J^{dt} = 8, 2 Hz, 2 H), 7.99 (m, 4 H), 8.09 (dt, J^{dt} = 8, 2 Hz, 2 H), 8.17 (d, J^d = 8 Hz, 2 H), 8.20 (d, J^d = 8 Hz, 2 H), 8.29 (d, J^d = 6 Hz, 2 H), 8.37 (d, J^d = 8 Hz, 2 H), 8.65 (d, J^d = 6 Hz, 2 H). ^{13}C NMR: (175 MHz, ACETONITRILE-d_3) δ ppm 163.4, 161.1,

158.8, 158.6, 158.2, 157.3, 154.7, 153.9, 152.8, 152.7, 152.3, 139.1, 138.6, 138.4, 138.3, 128.6, 128.3, 128.1, 127.9, 125.9, 125.4, 125.2, 124.4, 103.1, 49.8, 49.7, 48.8, 48.6, 23.3, 23.0. HRMS (ESI), m/z: 1617.20013 $[M\text{-}PF_6]^+$ ($C_{58}H_{58}N_{16}P_3F_{18}Ru_2$ requires 1617.20373), 736.11630 $[M\text{-}2PF_6]^{2+}$ ($C_{58}H_{58}N_{16}P_2F_{12}Ru_2$ requires 736.11950), 442.42360 $[M\text{-}3PF_6]^{3+}$ ($C_{58}H_{58}N_{16}PF_6Ru_2$ requires 442.42476), 295.57665 $[M\text{-}4PF_6]^{4+}$ ($C_{58}H_{58}N_{16}Ru_2$ requires 295.57738). Anal. Calc. for $C_{58}H_{58}N_{16}Ru_2P_4F_{24}$.$2H_2O$: C: 38.76; N: 12.47; H: 3.48. Found: C: 38.69; N: 12.35; H: 3.26.

X-ray diffraction studies:

Single crystals of **1**(***meso***), suitable for X-ray structure determination, were grown by slow vapour diffusion of diethyl ether into concentrated acetonitrile solution of **1**(***meso***). Diffraction data were collected on a Bruker SMART 6000 with Montel 200 monochromator, equipped with a rotating anode source for Cu Kα radiation. Cell refinement and data reduction were done using APEX2.[2] Absorption corrections were applied using SADABS.[3] Structures were solved by direct methods using SHELXS97 and refined on F^2 by full-matrix least squares using SHELXL97. All non-hydrogen atoms were refined anisotropically. Hydrogen atoms were refined isotropic on calculated positions using a riding model. For the crystal structure of **1**(***meso***), the highest difference peak is located 1.24 Å from atom Ru1. In addition, in **1**(***meso***) three more peaks with density around 1 e/Å^3 were present essentially 1.25 Å from Ru-atoms. The other Q peak of 0.81 e/Å^3 is due to rotational disorder of fluorine atom F12, and this small disorder was not taken into account for modelling.

Table T1. Crystallographic data for **1**(***meso***).(**2C_2H_3N**).

Compound	**1**(***meso***).(**2C_2H_3N**)
CCDC Number	964842
Formula	$[C_{58}H_{58}N_{16}Ru_2][4(PF_6)][2(C_2H_3N)]$
Mw (g/mol); $d_{calcd.}$(g/cm^3)	1843.33; 1.651
T (K); F(000)	150(2); 3704
Crystal System	Monoclinic
Space Group	Cc
Unit Cell:	
a (Å)	22.038(2)
b (Å)	14.0363(13)
c (Å)	25.925(3)
α (°)	90
β (°)	112.384(2)
γ (°)	90
V (Å^3); Z	7415.2(13); 4
θ range (°); completeness	3.87- 69.21; 0.995
R_{fle}:collec./indep.; R_{int}	108217/ 13608; 0.0597
μ (mm^{-1})	5.136
R1(F); wR(F^2); GoF(F^2)[a]	0.0382; 0.1011; 1.052
Residual electron density	0.980; -0.454
Flack parameter	0.1081 (0.0049)

[a]R1(F) based on observed reflections with I>2s(I) for **1(*meso*).(2C_2H_3N)**; wR(F^2) and GoF(F^2) based on all data for all compounds.

Table **T2**. Selected bond distances and angles of **1**(***meso***)**.(2**C_2H_3N**)**.

Compound	Distances (Å)		Angles (°)	
1.(2C_2H_3N**)**	N1-Ru1	2.089(3)	N1-Ru1-N9	84.57(12)
	N3-Ru1	2.069(3)	N3-Ru1-N4	78.87(12)
	N4-Ru1	2.059(3)	N5-Ru1-N6	79.30(14)
	N5-Ru1	2.053(3)	N2-Ru2-N16	84.34(12)
	N6-Ru1	2.078(3)	N10-Ru2-N11	79.23(13)
	N9-Ru1	2.096(3)	N12-Ru2-N13	79.49(17)
	N2-Ru2	2.085(3)		
	N10-Ru2	2.063(3)		
	N11-Ru2	2.058(3)		
	N12-Ru2	2.064(4)		
	N13-Ru2	2.061(3)		
	N16-Ru2	2.096(4)		
	C4-N7	1.402(5)		
	N7-C51	1.402(5)		
	N8-C51	1.347(5)		
	N9-C51	1.304(5)		
	C2-N14	1.394(5)		
	N14-C58	1.406(5)		
	N15-C58	1.343(6)		
	N16-C58	1.290(6)		

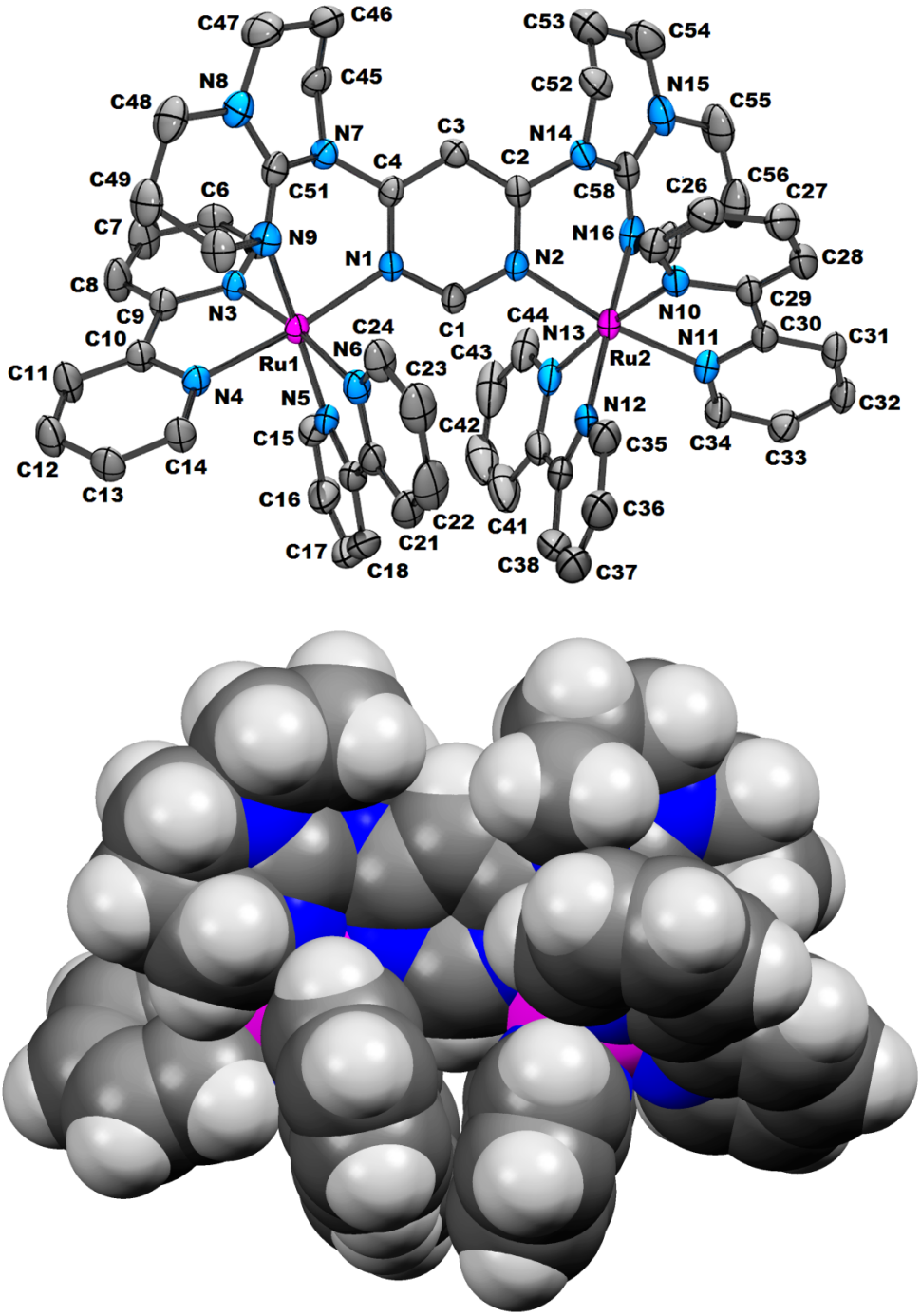

Fig. S1 View of ortep diagram of **1**(***meso***) (ellipsoids correspond to 50% probability level), with complete labeling (top) and spacefill model of **1**(***meso***) (bottom), along the perpendicular plane of central pyrimidine ring, showing the π-π interaction of the bpy units, favoring for the diastereoselective formation of ΛΔ (or ΔΛ)-isomer over ΔΔ or ΛΛ-isomer.

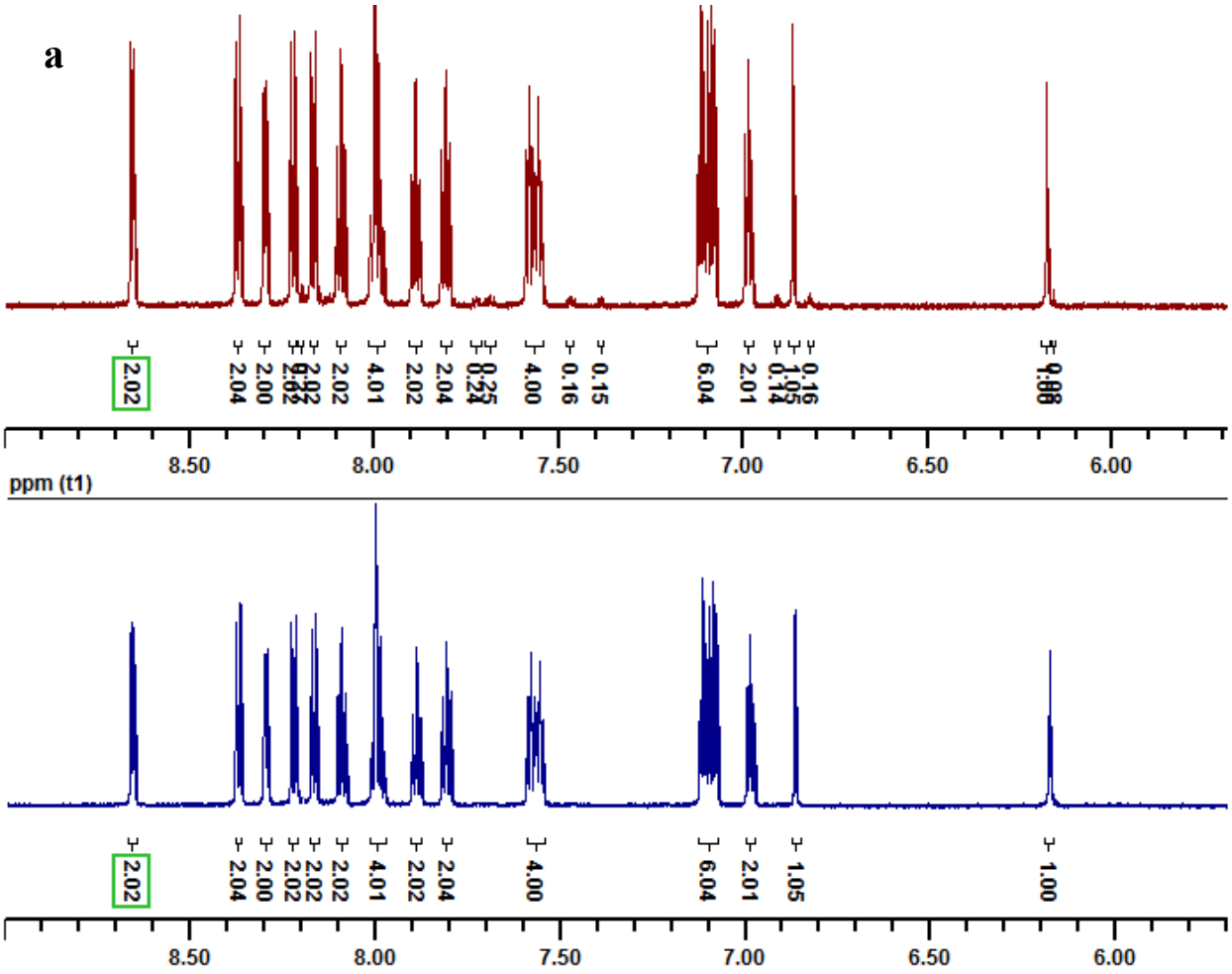
a
2.02
2.04
2.00
2.02
2.02
4.01
2.02
2.04
4.00
0.16
0.15
6.04
2.01
1.05
1.00
8.50
8.00
7.50
7.00
6.50
6.00
ppm (t1)

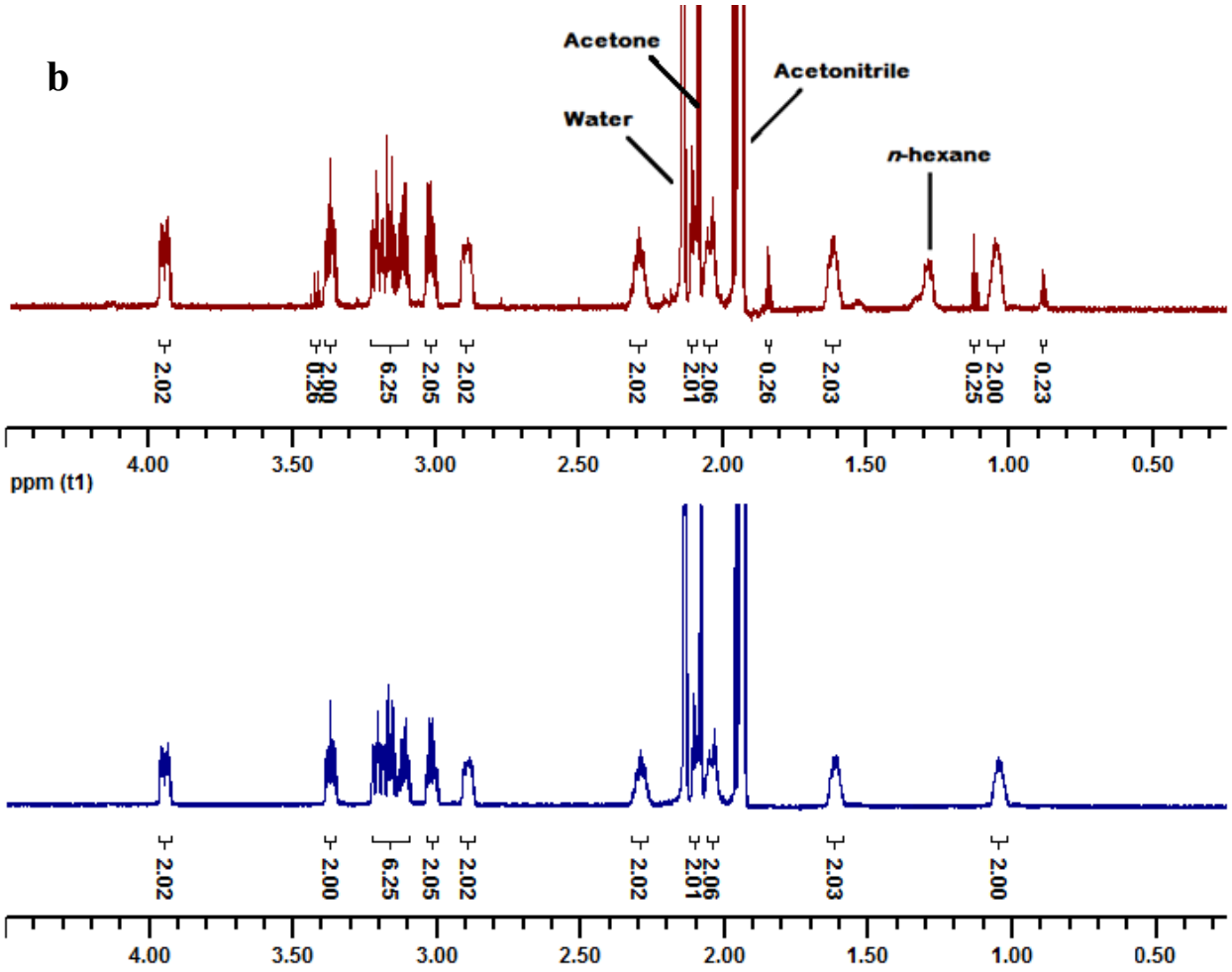

Fig. S2: Comparison of ^{1}H NMR of **1**(***meso***) (as its crystalline form) with the product obtained after reaction ii (see Scheme 1 in main text) at 700 MHz in CD_3CN at room temperature; (a) top - aromatic region of product obtained after reaction ii, bottom - aromatic region of **1**(***meso***), (b) top - aliphatic region of product obtained after reaction ii, bottom - aliphatic region of **1**(***meso***).

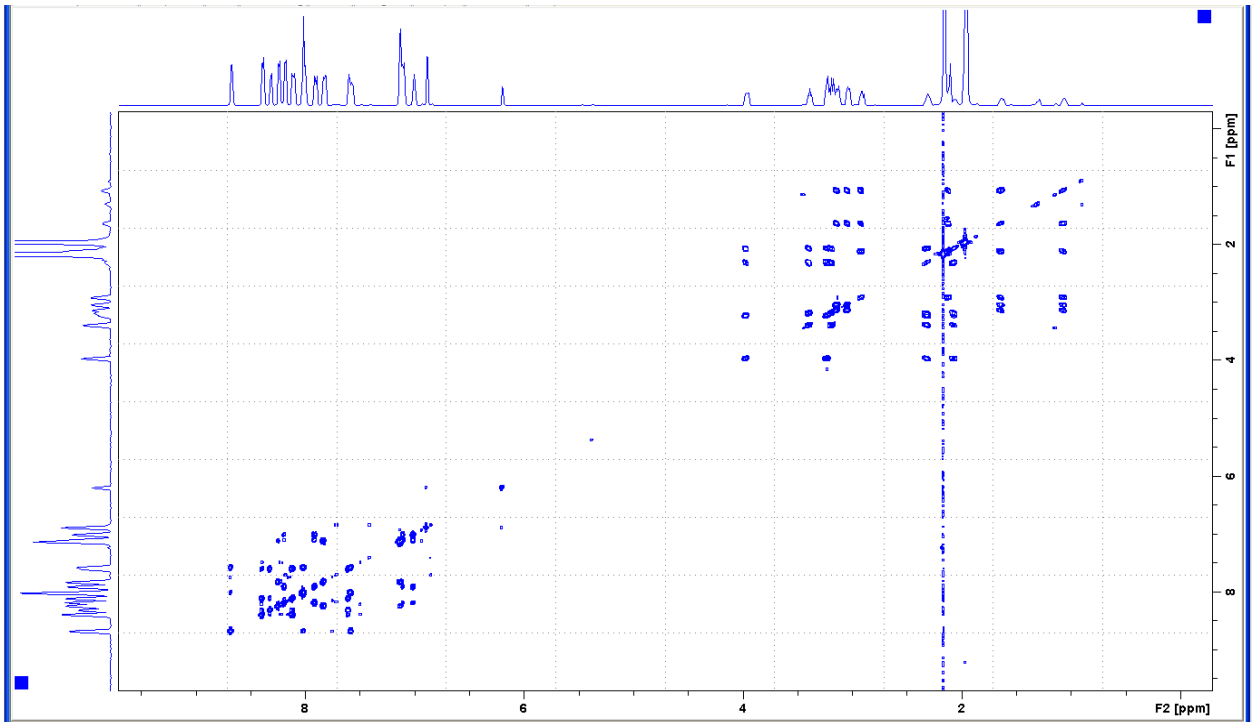

Fig. S3: ^{1}H COSY-NMR of the product obtained after reaction ii (see Scheme 1 in main text) in CD_3CN at 700 MHz at room temperature.

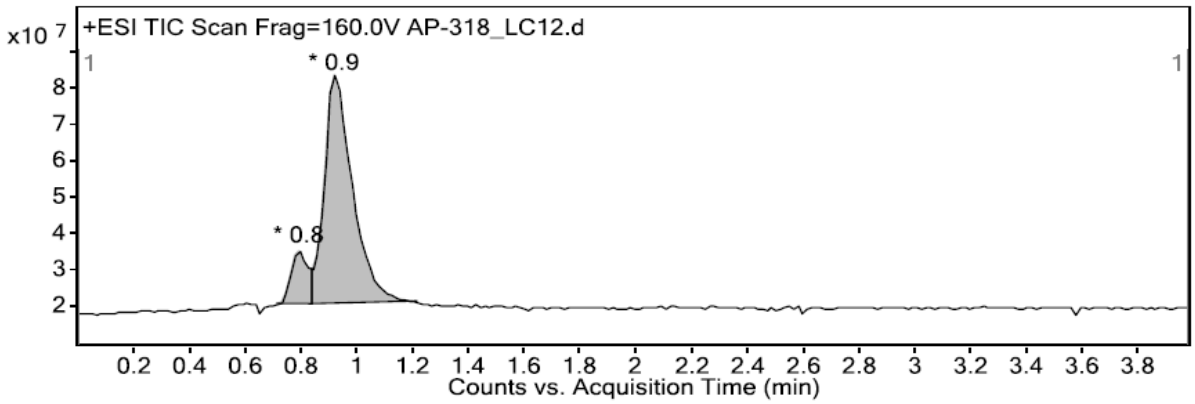

Integration Peak List

RT	Height	Area
0.8	14722971	68546361
0.9	62945285	443168110

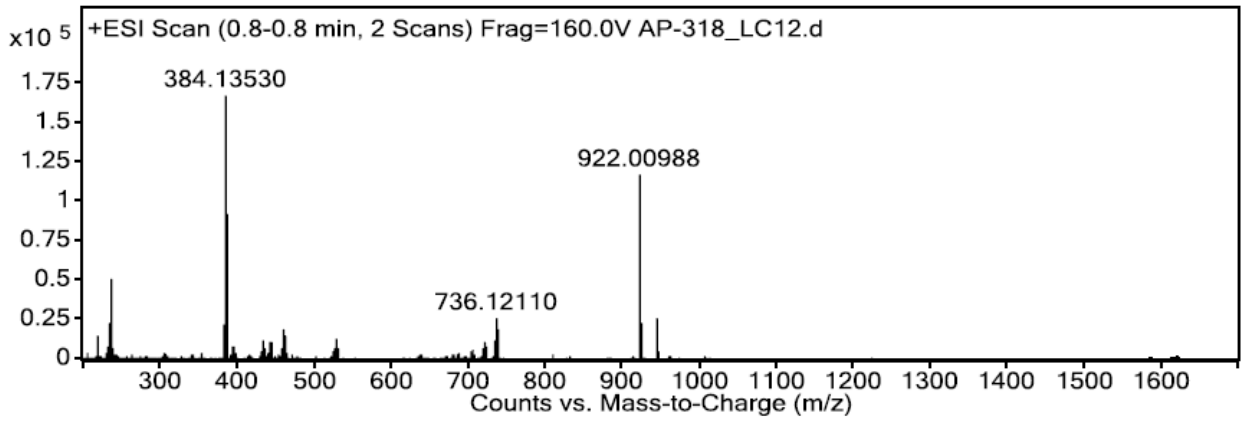

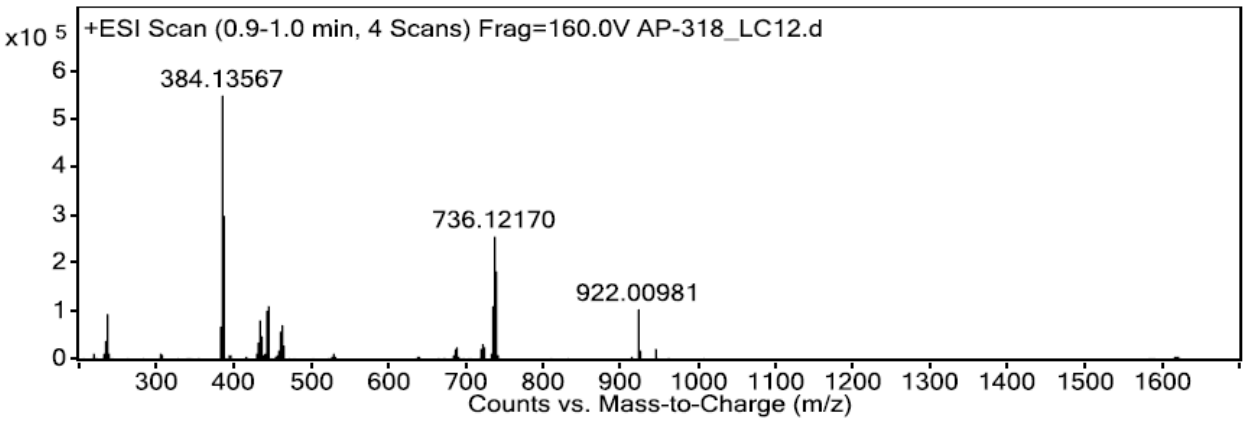

Fig. S4 LC-MS of reaction ii (see Scheme 1 in main text) conataing 2:13 mixture of *rac*:*meso* isomer, using an achiral support, showing the separation of the *rac*-ΔΔ or ΛΛ-isomer (retention time at 0.8 min) and the *meso*-ΔΛ or ΛΔ-isomer (retention time at 0.9-1.0 min).

Table T3. Electrochemical data for **L1** and **1**(***meso***) and some reference compounds.

Compound		$E_{1/2}$(ox)[a]		$E_{1/2}$(red)[a]					$\Delta E_{1/2}$[b]	ΔE_{ox}[c]	K_c (x10^3)[d]
L1		1.18 (136)	0.89[e] (irr)						------	------	------
1(**meso**)		1.00 (68)	0.84 (84)	-1.36 (68)	-1.46 (65)	-1.62 (66)	-1.78 (68)	-1.87 (69)	2.20	0.160	0.506
$[Ru(bpy)_2$(2-(hpp) pyrimidine)$][(PF_6)_2]$[f]			0.75 (90)	-1.42 (62)	-1.63 (133)	-1.96 (145)			2.17		------
$[Ru(bpy)_3][(PF_6)_2]$[g]			1.26	-1.33	-1.51	-1.77			2.59		------
$[\{Ru(bpy)_2\}_2(\mu$-L3)$][(PF_6)_4]$[g]	meso										1.760
	rac										1.510
$[\{Ru(bpy)_2\}_2(\mu$-L4)$][(PF_6)_4]$[h,i]		1.540	1.370	-0.53	-1.08	-1.50	-1.81		1.900	0.170	0.747
$[\{Ru(bpy)_2\}_2(\mu$-L5)$][(PF_6)_4]$[g]	meso	1.530	1.370	-0.566	-1.190	-1.614			1.936	0.160	0.506
	rac	1.518	1.350	-0.582	-1.214	-1.610			1.932	0.168	0.690
$[\{Ru(bpy)_2\}_2(\mu$-L6)$][(PF_6)_4]$[g]	meso	1.566	1.354	-0.734	-1.230	-1.578			2.088	0.212	3.830
	rac	1.554	1.342	-0.738	-1.250	-1.590			2.080	0.212	3.830
$[\{Ru(bpy)_2\}_2(\mu$-L7)$][(PF_6)_4]$[j]	meso	1.846	1.486	-0.510					1.996	0.36	1220
	rac	1.846	1.510	-0.562					2.072	0.336	478
$[\{Ru(bpy)_2\}_2(\mu$-L8)$][(PF_6)_4]$[j]	meso	1.702	1.438	-0.722					2.160	0.264	29
	rac	1.679	1.421	-0.658					2.079	0.258	23
$[\{Ru(bpy)_2\}_2(\mu$-L9)$][(PF_6)_3]$[k]	meso	1.286	0.946	-1.510	-1.670				2.456	0.340	560
	rac	1.306	0.946	-1.499	-1.658				2.445	0.360	1200
$[\{Ru(bpy)_2\}_2(\mu$-L10)$][(PF_6)_3]$[g]	meso	1.154	0.842	-1.514	-1.742	-2.218			2.356	0.312	188
	rac	1.194	0.850	-1.490	-1.754	-2.238			2.340	0.349	652

[a]Potentials are in volts vs SCE for acetonitrile solutions, 0.1 M in $[n\text{-}Bu_4N]PF_6$, recorded at 25 ± 1 °C at a sweep rate as mentioned in experimental section (the ferrocene/ferrocenium couple occurred at +310 mV *vs.* SCE, except for the first three compounds in this table, which occurred at +395 mV *vs.* SCE). The difference between cathodic and anodic peak potentials (millivolts) is given in parentheses. [b]Difference between the first oxidation and first reduction potentials (volt). [c]Difference between the first and second oxidation potentials (volt). [d]$K_c = \exp\{\Delta E_{ox}F/RT\}$, where F/RT takes the value 38.92 V^{-1} at 298 K. [e]Irreversible; potential is given for the anodic wave. [f]From ref. 4. [g]From ref. 5. [h]From ref. 6. [i]From ref. 7. [j]From ref. 8. [k]From ref. 9.

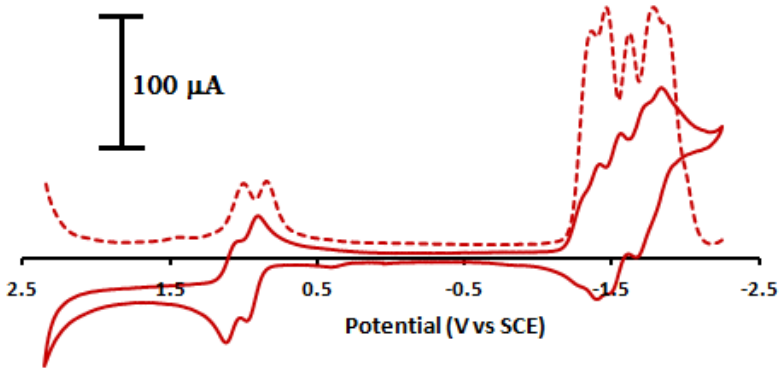

Fig. S5. Cyclic voltammogram (solid line) and differential pulse voltammogram (dotted line) of **1**(***meso***) in dry, degassed CH_3CN, recorded at a scan rate of 25 and 20 mV/s, respectively.

Table T4. UV-Vis absorption data of **L1** and **1**(***meso***).

Compound	λ_{max}, nm ($\varepsilon x10^3$, $M^{-1}cm^{-1}$)				
L1	237 (29.9)	285 (9.9)			
1(***meso***)	244 (25.2)	289 (51.5)	345 (7.2)	368 (7.0)	470 (6.8)

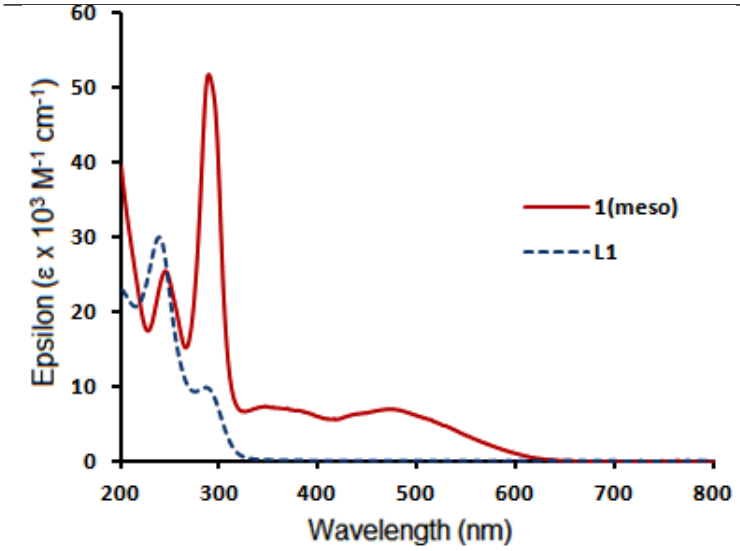

Fig. S6. Electronic absorption spectra of **L1** and **1**(***meso***), at ambient temperature in dry acetonitrile.

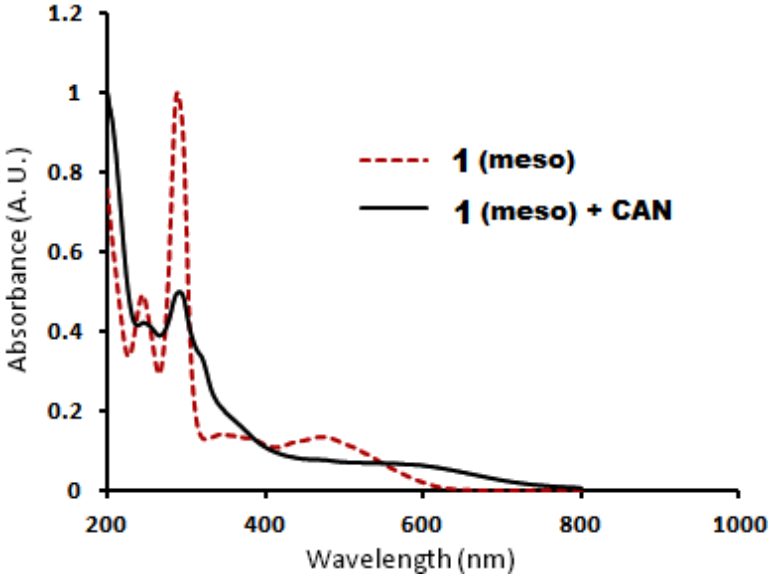

Fig. S7. Electronic absorption spectra of **1**(***meso***) and **1**(***meso***) + equimolar amount of cerium ammonium nitrate (**CAN**), at ambient temperature in dry acetonitrile.

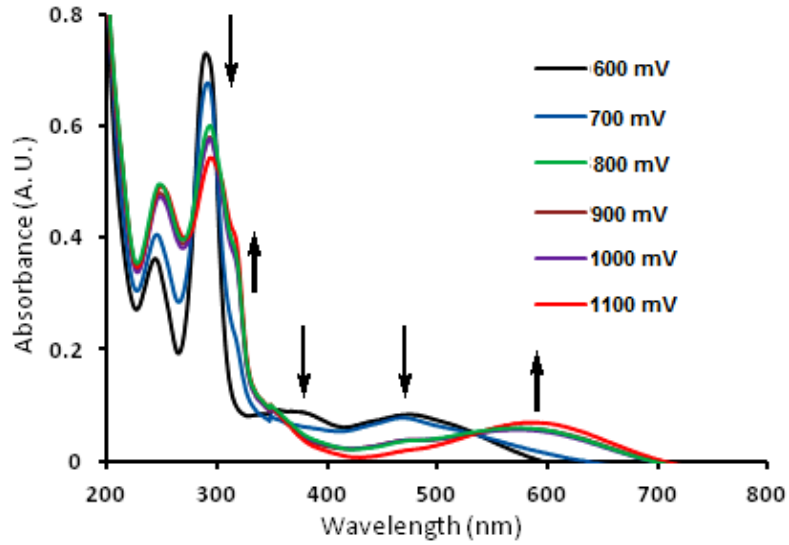

Fig. S8. Spectral progression of the oxidation reaction (**1***meso*)$^{4+}$ to (**1***meso*)$^{5+}$ to (**1***meso*)$^{6+}$ with increasing applied potential.

References:

1. G. Sprintschnik, H. W. Sprintschnik, P. P. Kirsch, D. G. Whitten, *J. Am. Chem. Soc.*, 1977, **99**, 4947.
2. *APEX2 (2007) version 2.4-0; Bruker Molecular Analysis Research Tool.* Bruker AXS Inc., Madison, WI 53719-1173.
3. G. M. Sheldrick (1996). *SADABS*, Bruker Area Detector Absorption Corrections. Bruker AXS Inc., Madison, WI 53719-1173.
4. A. K. Pal, S. Nag, J. G. Ferreira, V. Brochery, G. L. Ganga, A. Santoro, S. Serroni, S. Campagna, G. S. Hanan, *Submitted*.
5. J. W. Slater, D. M. D'Alessandro, F. R. Keene, P. J. Steel, *Dalton Trans.*, 2006, **16**, 1954.
6. G. Denti, S. Campagna, L. Sabatino, S. Serroni, M. Ciano, V. Balzani, *Inorg. Chem.*, 1990, **29**, 4150.
7. S. Ernst, V. Kasack, W. Kaim, *Inorg. Chem.*, 1988, **27**, 1146.
8. C. Richardson, P. J. Steel, D. M. D'Alessandro, P. C. Junk, F. R. Keene, *J. Chem. Soc*., *Dalton Trans*., 2002, 2775.
9. C. Richardson, C. M. Fitchett, F. R. Keene, P. J. Steel, *Dalton Trans.*, 2008, 2534.